

# SimNet: Computer Architecture Simulation using Machine Learning

Lingda Li, Santosh Pandey<sup>†</sup>, Thomas Flynn, Hang Liu<sup>†</sup>, Noel Wheeler<sup>§</sup>, Adolfo Hoisie  
Brookhaven National Laboratory, <sup>†</sup>Stevens Institute of Technology, <sup>§</sup>Laboratory for Physical Sciences  
{lli, tflynn, ahoisie}@bnl.gov, {spande1, hliu77}@stevens.edu, nwheeler@lps.umd.edu

## ABSTRACT

While cycle-accurate simulators are essential tools for architecture research, design, and development, their practicality is limited by an extremely long time-to-solution for realistic problems under investigation. This work describes a concerted effort, where machine learning (ML) is used to accelerate discrete-event simulation. First, an ML-based instruction latency prediction framework that accounts for both static instruction/architecture properties and dynamic execution context is constructed. Then, a GPU-accelerated parallel simulator is implemented based on the proposed instruction latency predictor, and its simulation accuracy and throughput are validated and evaluated against a state-of-the-art simulator. Leveraging modern GPUs, the ML-based simulator outperforms traditional simulators significantly.

## 1. INTRODUCTION

Adopted extensively in computer architecture research and engineering, cycle-accurate simulators enable new architectural ideas, as well as design space exploration. Unfortunately, cycle-accurate simulation is extremely computationally demanding, significantly diminishing its practicality and applicability at system and full application scales. Typical simulations using the state-of-the-art gem5 simulator [7] execute at speeds of hundreds of kilo instructions per second on modern CPUs, about four to five orders of magnitude slower than native execution. More detailed simulators, such as gate or register transistor level, further decrease simulation speed. In this context, it would require extended periods of time to execute real-world applications that may execute trillions of instructions. To expand the practical limits of traditional simulation, design space exploration necessitates a multitude of simulations across various applications and design parameters under consideration.

Although simulation speed has steadily improved through statistic methods [39, 45], software engineering optimizations [15, 28, 35], and parallelization [16, 34], a need clearly exists for more significant advances—particularly given that the complexity of architectures, applications, and design space all have increased significantly, leading to more simulation demand. At the moment, in a typical simulation project, simplifications of architecture and application workloads are needed, such as utilization of a fixed set of benchmarks/microbenchmarks. However, there are few options to optimize speed without sacrificing accuracy. Of those,

enabling and taking advantage of increased parallelism is a somewhat promising direction, thanks to the availability of massively parallel accelerators. However, highly irregular behaviors and frequent interactions between different components in the simulator limit the viability of parallelism.

This work proposes an alternative path to accelerate architectural simulation compared to traditional discrete-event simulation that still maintains the same level of simulation accuracy. Hence, we introduce SIMNET, a new instruction-centric simulation framework that decomposes program simulation into individual instruction latency and uses tailored machine learning (ML) techniques for instruction latency prediction. Program performance is obtained by combining the latency prediction results of all executed instructions. A significant advantage of SIMNET is its ability to leverage state-of-the-art massively parallel accelerators (e.g., GPU; TPU [18]) for much higher simulation throughput, which can be attributed to well-optimized ML infrastructures [3, 27, 42].

Using ML for specific performance prediction tasks is significant and growing. Considerable research has been done to predict program performance [4, 5, 6, 14, 22, 26, 47]. The major limitation of these methods is they are program/input dependent, which means ML models need to be trained for distinct program and input combinations. As a result, their flexibility is limited compared to simulation-based approaches. Ithemal [24] represents the closest related work to this effort, proposing a long short-term memory (LSTM) model to predict the execution latency of static basic blocks. While being similar to our work as an instruction-level simulation approach, Ithemal differs in three specific areas: 1) it targets a simplified processor model without branch prediction and cache/memory hierarchies; 2) it focuses on the performance prediction of basic blocks with a handful of instructions, while real-world simulation executes billions or trillions of instructions; and 3) it simulates instructions at a pace of thousands of instructions per second, which is significantly slower than traditional simulators. As a result, Ithemal can neither simulate real-world processors nor programs. In our work, we tackle all of these problems to establish the first ML-based architecture simulation framework.

This work’s contributions to the science and practice of simulation include:

- We propose to use ML technologies to predict instruction latency. The ML-based predictor accounts for both static instruction properties and dynamic processor be-

haviors in the input (Section 2). Extensive ML models are evaluated for this task to balance between the prediction accuracy and speed (Section 3). Our exploration demonstrates that deep convolutional neural networks (CNNs) are competent to learn complex processor behaviors, such as cache accesses, and to predict instruction latency.

- We propose an instruction-centric architecture simulation framework that is built upon ML-based instruction latency predictors (Section 4). Evaluated using a realistic benchmark suite and on full microprocessor architectures, we demonstrate that the proposed approach simulates programs faithfully compared with the cycle-accurate simulator that it learns from. To the best of our knowledge, the proposed framework is the first of its kind and could set the stage for developing alternative tools for architecture researchers or engineers.
- We also prototype a GPU-accelerated ML-based simulator (Section 4.3). It improves the simulation throughput up to  $18.5\times$  compared to its traditional counterpart.

**Scope of the Paper.** This paper focuses on the simulation of **out-of-order superscalar CPUs**, which employ technologies such as multi-issue, out-of-order scheduling and speculative execution to exploit instruction-level parallelism. We believe the proposed simulation methodology also is applicable to other processor architectures, which usually are less complicated to simulate. In addition, we constrain the scope to the **prediction of program performance** and **single-thread program simulation**, leaving multiple-thread/program simulation for future work. Traditional simulators also produce other metrics, such as energy consumption, to help extract more insights. While it is reasonable to assume the proposed method is applicable to their prediction as well, these metrics are not considered in this work.

## 2. ML-BASED SIMULATION FRAMEWORK

### 2.1 Cycle-accurate Simulation Background

Computer architects use software cycle-accurate simulators extensively in the early design stage because it often is prohibitively expensive to implement real hardware prototypes in terms of both time and financial costs. Simulators take one or a set of programs as their inputs. The simulator explores the inputs instruction by instruction to simulate the interaction between hardware and software, and it reports the performance metrics and other statistics of interest as the output when all instructions finish execution.

Internally, traditional simulators are composed of various software modules that mimic the behavior of different hardware components. Hardware system simulation is achieved by simulating individual components within it and their interactions. We call these simulators, *component-centric*.

A promising option to optimize the performance of these component-centric simulators is to employ modern parallel processors that are widely available, such as GPUs. However, traditional simulators are extremely difficult to parallelize because the heterogeneous nature of distinct components makes

it difficult to leverage parallel processors that require massive and regular parallelism. In addition, there are frequent interactions between components, which introduce a large amount of communications between processing units.

### 2.2 Instruction-centric Simulation

To avoid the intrinsic limitations of component-centric simulators, we argue that an *instruction-centric* simulator is better suited for the task, and recent developments in ML technology have paved the way for a successful implementation. The instruction-centric simulator’s key role is to predict the latency of individual instructions then infer the program performance based on these prediction results. We propose to use ML for the task of instruction latency prediction.

### 2.3 Factors that Determine Instruction Latency

Successful latency prediction by an ML model is contingent upon capturing all factors that impact latency in its design and implementation. These factors can be summarized into three categories.

**Static Instruction Properties.** These properties describe the basics of an instruction, including the operation types, source/destination registers, etc. They guide how an instruction is executed in a processor. For instance, the type of instruction determines its computation resource (e.g., function units; register files) and synchronization (e.g., memory barriers) requirements. These static properties can be extracted from the instruction encoding directly.

**Architecture Configuration.** Architecture configuration represents the static properties of the simulated architecture. It includes both quantifiable properties, such as the number of physical registers and the L1 data cache size, and immeasurable properties, such as the instruction scheduling strategy and memory consistency requirements.

**Dynamic Behaviors.** Along with static instruction and architecture properties, the latency of an instruction largely depends on its runtime behaviors during execution, which are decided by the hardware states in the component-centric simulation. We refer to these states as *contexts* and further distill them into two categories.

*Instruction Context:* Many contexts relate to other concurrently running instructions in the processor, referred to as *instruction context* in this paper. For example, if an instruction depends on the result produced by a previous instruction that has not yet finished, it must wait until the result is ready. A less intuitive example is whether a memory access results in a miss statue history register (MSHR) hit or a miss in the cache belongs to the instruction context. Recall that MSHR requests are waiting for their responses from the lower memory hierarchy. As a result, instructions that generate these pending requests have not yet been completed. Therefore, an MSHR hit indicates that another co-running instruction accesses the same cache line. The processor capacity decides the maximal number of instructions in the instruction context.

*History Context:* The remaining hardware contexts depend on events that happened in the long-term execution history. Cache, translation lookaside buffer (TLB), and branch predictor states belong to this category. For example, whether a memory load hits in the L2 cache depends on when the same cache line was last accessed, and branch prediction results

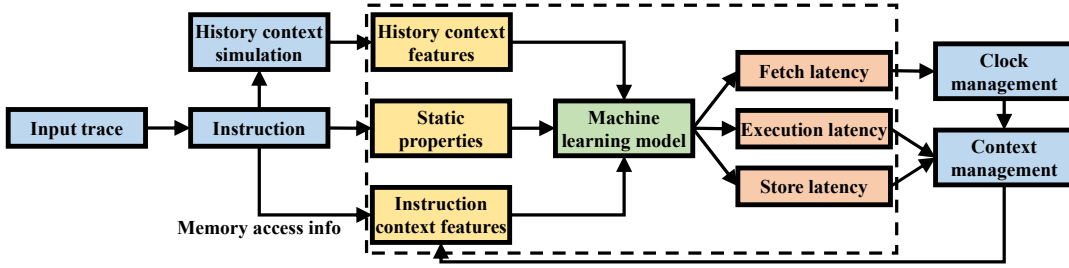


Figure 1: ML-based simulation framework. The ML-based instruction latency predictor is shown in green (Section 3), and its input and output are in yellow and orange, respectively (Section 2.4). Other simulator components are in blue (Section 4).

Impact Factor	Features
Static properties	13 operation features (function type, direct/indirect branch, memory barrier, etc.); 14 register indices (8 sources and 6 destinations)
Instruction context	27 static properties; 14 history context features; 1 residence latency; 1 execution latency; 1 store latency; 5 memory dependency flags to indicate if it shares the same instruction/data address/cache line/page with the current instruction
History context	1 branch misprediction flag; 1 fetch depth; 3 fetch table walking depths; 2 fetch caused writebacks; 1 data access depth; 3 data access table walking depths; 3 data access caused writebacks

Table 1: Input features for various instruction latency impact factors.

hinge on the branch execution history. Traditional simulators employ lookup tables (e.g., cache tag array; branch target predictor) to keep track of such states. We refer to them as *history context*.

## 2.4 ML-based Instruction Latency Prediction

With these impact factors, we are ready to build an instruction latency prediction framework as shown inside the dashed box of Figure 1. An ML-based instruction latency predictor (the green box) is the center of the framework, which captures the architecture configuration. Its inputs (yellow boxes) take into account the other aforementioned impact factors, static instruction properties and context (both instruction and history contexts). Table 1 summarizes the input features to model various impact factors, and we will introduce them in detail herein. While many ML frameworks adopt one-hot encoding for individual input features, we choose not to do so for smaller input size and faster prediction speed. The framework aims to balance between two competing goals: to predict instruction latency *accurately* and *swiftly*.

**Modeling Static Instruction Properties.** The second row of Table 1 lists the static instruction properties used as the input features of the ML model, including 13 operation flags and 14 source and destination register indices. They are well known to computer architects.

**Modeling Instruction Context.** To account for the impact of concurrently running instructions, the key is to model their *relationships* with the to-be-predicted instruction. Such relationships include resource competition, register dependency, and memory dependency. We name these concurrently running instructions, *context instructions*. Formally, the context instructions are those instructions present in the processor when a particular instruction is about to be fetched. In theory, instructions issued after the current instruction can also influence its execution. However, these cases are rare, and we only include previous instructions in the context for practicality reasons. The third row of Table 1 shows input features per context instruction.

For resource competition and register dependency, it is sufficient to provide the static properties of context instructions (i.e., their operation features and register indices). The ML model is responsible for deducing the resource competition using their operation features and the register dependency by comparing register indices.

To model the memory dependency (including instruction fetch and data access), one solution is to provide memory access addresses as parts of input features. Unlike register indices, memory access addresses spread across a much wider range in a typical 64-bit address space. Thus, having addresses as input would slow down the ML model prediction speed. Instead, we extract the memory dependency by explicitly comparing the memory access addresses of the current instruction with those of context instructions and generate several *memory dependency flags* as input features. For instance, we compare their program counters (PCs) to identify if they fall into the same instruction cache line. This PC dependency flag presumably helps with fetch latency prediction as instructions that share the same instruction cache line can be fetched together. Similarly, there are dependency flags to indicate if data accesses share the same address, cache line, and page.

In addition, we introduce several features to capture the temporal relationship between instructions. Particularly, we include the number of cycles it has stayed in the processor (i.e., residence latency), how long it takes to complete execution (i.e., execution latency), and the memory store latency (i.e., store latency) if applicable. The latter two are provided by the ML model output, which will be introduced shortly.

**Modeling History Context.** History context reflects the hardware states that depend on long-term historical events, and it includes caches, TLBs, and branch predictors. It is impractical to either capture the history context within the ML model or directly have it as the input because it includes a huge amount of information. Considering a 2MB cache with 64B cache lines as an example, we will need  $\sim 5B$  per cache line to store its address tag, etc. Totally, a 2MB cache requires

storing at least  $2\text{MB} \div 64\text{B} \times 5\text{B} = 160\text{KB}$  of information to simulate it accurately. The total history-context-related information is much larger given all history context. It is prohibitively expensive and inefficient to allow the ML model to handle such large amounts of information directly.

Fortunately, the majority of history context impacts can be captured using a small number of intermediate results. For a memory access, the cache/TLB level in which it gets hit roughly determines its latency. Similarly, whether or not a branch target is predicted correctly determines the impact of a branch.

Therefore, we propose to simulate history context components explicitly to obtain these intermediate results (i.e., *history context simulation*), which are passed to the ML model as input features. History context simulation alleviates the burden on ML models significantly. As shown in the last row of Table 1, a branch misprediction flag is obtained for a branch instruction. A *depth* feature is used for each memory access to indicate which level of the cache/TLB hierarchy satisfies the request. All instructions require fetch access and fetch table walking depths, and load/store instructions need data access and data table walking depths, e.g., a load request that hits in the L2 cache has a depth of 2. The numbers of cache writebacks generated are also included in input features to capture their impacts.

Note that obtaining these intermediate results mostly involves table lookups (e.g., cache tag array; branch direction predictor). Detailed structures, such as pipeline and MSHR, are not needed in the history context simulation, whose impacts are captured by the ML model. Therefore, the history context simulation is lightweight and has negligible impact on the overall performance.

**ML Model Input Summary.** In total, each context instruction has 50 features, and the to-be-predicted instruction has 47 features. For alignment purposes, we pad the to-be-predicted instruction features with three zeros, to have an equal number of 50 features. Together, the ML model input includes  $50 \times (\# \text{ context instructions} + 1)$  features.

**ML Model to Capture Architecture Timing Details.** We train the ML model to learn the architecture timing details. Section 3 will introduce the details of ML models and the training procedure.

In this work, an ML model is trained to estimate the instruction latency under a certain architecture configuration. The limitation of having a corresponding model per architecture configuration is the need to retrain for different architecture configurations. As such, this has less flexibility. The reason behind our choice is three-fold. 1) Because the history context simulation is employed to estimate the impact of caches, TLBs, and branch predictors, most parameters of these modules are configurable without the need for retraining. 2) Many configuration parameters are not measurable (e.g., the instruction scheduling strategy). It is not clear how to provide them as input to the ML model. Thus, it is reasonable to train separate ML models for different choices of such parameters. 3) Most measurable parameters are standardized and of little interest for computer architecture research. Nevertheless, we plan to explore using some measurable parameters (e.g., reorder buffer size) as input to the ML model in the future. In this way, we can explore the impact of the selected

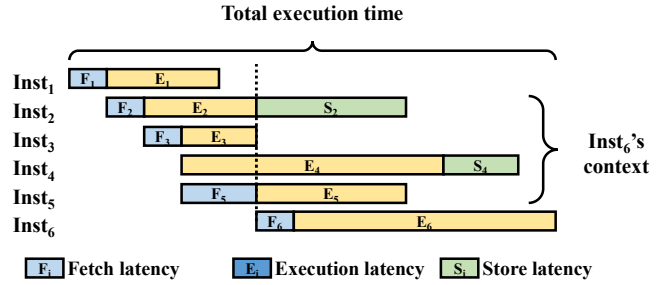


Figure 2: From instruction latency to program execution time.

parameters quickly without model retraining.

**ML Model Output.** In Figure 1, the ML model is designed to predict three types of latency per instruction: fetch, execution, and store. Fetch latency represents how long an instruction needs to wait to enter the processor after the previous instruction is fetched. It is affected by both its instruction fetch request state and context instructions (e.g., when it follows a mispredicted branch). Execution latency represents the time interval from when an instruction is fetched to when it finishes execution and is ready to retire from the reorder buffer (ROB). Note the ROB retire latency is larger because the ROB retires instructions in order. For store instructions, they write memory after being retired from the ROB. The store latency is used to represent the latency from when a store instruction is fetched to when it completes memory write (i.e., when it is ready to retire from the store queue (SQ)).

## 2.5 From Instruction Latency Predictor to Simulator

The program execution time can be calculated by leveraging the fact that instruction fetch, instruction retire from ROB and SQ happen in order. Figure 2 illustrates how to calculate program execution time using the output latency of an ML-based predictor. Note that the fetch latency could be 0 in cases when multiple instructions are fetched together (e.g., Inst4). We observe the execution time  $\mathcal{E}$  of a program can be computed as

$$\mathcal{E} = \left( \sum_{i=1}^n F_i \right) + \Delta, \quad (1)$$

where  $n$  is the total number of simulated instructions,  $F_i$  represents the fetch latency of the  $i$ th instruction, and  $\Delta$  is the amount of time from when the last instruction is fetched to when all instructions exit the processor. When  $n$  is large enough, the total execution time is dominated by the accumulated fetch latency, and  $\Delta$  is negligible. This equation provides the foundation for the proposed ML-based simulator, and Section 4 will introduce its implementation in detail.

Although execution and store latency do not directly play a significant role in the program execution time calculation, it is important to predict them for two reasons. First, they determine the life span of an instruction and how long it stays in the context. In Figure 2, when Inst6 is about to be fetched (vertical black-dotted line), Inst1 has retired, and Inst2~5 are still in the processor based on their execution and store latency. Therefore, Inst2~5 are the context instructions of Inst6.

Second, having the execution and store latency of context instructions in the input helps improve the prediction accuracy. Recall that they are parts of the instruction context features as shown in Table 1. For example, if a branch is mispredicted, its execution latency will decide the fetch latency of the next instruction.

### 3. ML-BASED LATENCY PREDICTOR

#### 3.1 Model Exploration

The first question we would like to answer is what kinds of ML models are suitable for instruction latency prediction. ML models, especially deep neural network models, have proven to be excellent function approximators in many domains, from computer vision to scientific computing [17, 37, 41, 43]. In the computer architecture simulation case, the goal is for the ML neural network to accurately model the instruction latencies on architectures under consideration. Due to the complexity of this task, we anticipate (and will later show) that deep neural network models are required to model modern computer architectures accurately.

**Sequence-oriented Models.** The ML-based instruction latency predictor processes instructions one by one in their execution order. Similar to natural language processing (NLP), where inputs are word sequences, in the case of ML-based architecture simulation, instruction sequences are processed. Therefore, an attractive option is to apply models designed to process sequences, such as recurrent neural networks [33], LSTM [13], and transformer [43], for instruction latency prediction. Ithetal [24] follows this strategy and adopts LSTM to predict basic block latency. However, these NLP models usually have long inference latency, resulting in slow simulation speed. Moreover, they are designed to account for the impact of a longer history because every word that appears earlier matters to the semantic meaning of an article or speech. In the instruction latency prediction case, the number of context instructions is limited by the processor capacity, and we do not need to consider instructions that have exited the processor.

**Deep Convolutional Neural Network Models.** Deep CNN models have shown great success in computer vision [12, 21, 41], where convolution kernels learn and recognize the spatial relationship between pixels. In our instruction latency prediction setting, learning the temporal relationship between the to-be-predicted instruction and context instructions is crucial, and convolution between instructions could help achieve this. Compared with fully connected networks, another important benefit of CNN is it significantly reduces the number of to-be-learned parameters and is much easier to achieve convergence during training. Therefore, we choose deep CNNs for our instruction latency predictor.

#### 3.2 Neural Network Architecture

Figure 3 illustrates the proposed CNN architecture.  $Inst_0$  represents the instruction to be predicted, and the ML model outputs  $F_0$ ,  $E_0$ , and  $S_0$ , which are its predicted fetch, execution, and store latency, respectively. Without loss of generality, Figure 3 shows three context instructions,  $Inst_{1,2,3}$ .

**Input Organization.** As introduced in Section 2.4, every

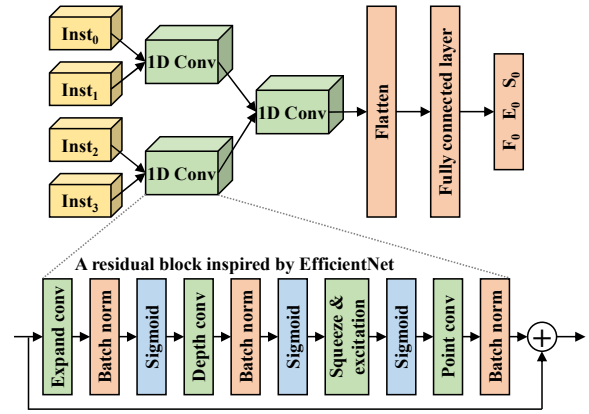


Figure 3: Neural network architecture illustration.

instruction includes 50 features. We organize instructions in a one-dimensional (1D) array by their execution order and have their features as channels, in CNN terminology. Using computer vision as an analogy, instructions correspond to pixels, except they are 1D instead of two-dimensional (2D), and instruction features correspond to RGB (red, green, and blue) channels. This input organization facilitates convolutional operations to reason the relationship between instructions. Again, it is analogous to reasoning the shape composed by pixels in computer vision.

**Instruction Convolution.** Because the input is organized in a 1D array, we perform 1D convolution. We organize the convolutional layers in a hierarchical way, where the first layer captures the relationship between temporally adjacent instructions, and subsequent layers integrate the impact of further away instructions. In Figure 3, the impact of  $Inst_1$  to  $Inst_0$  is captured in the first layer, and the impact of  $Inst_3$  is incorporated in the second layer. This hierarchical design prioritizes the impact of temporally closer context instructions while penalizing the influence of more distant instructions. For instance, if a source register of  $Inst_0$  is the destination register of both  $Inst_1$  and  $Inst_3$ ,  $Inst_0$  only has to wait for  $Inst_1$  where a true read after write dependency exists.

In our default design, each convolution layer includes a convolution operation followed by an activation operation. An alternative is to use a residual block as shown at the bottom of Figure 3, which facilitates the training of deeper CNNs [12]. In this work, we design a residual block with architecture inspired by the state-of-the-art computer vision model, EfficientNet [40, 41].

Empirically, we find the following CNN design principles work well for instruction latency prediction. First, the inputs of different convolutional operations have no overlap in contrast to computer vision CNNs. For example, we do not convolve  $Inst_1$  and  $Inst_2$  in Figure 3. In this way, the impact of a context instruction is integrated only once. Second, a convolution kernel size of 2 is always used to account for only two adjacent inputs, which reduces the complexity. Combined with the first principle, it means all convolutional layers have the uniform kernel and stride size, 2.

The output of the last convolutional layer is flattened then used as the input of two fully connected layers. At the end,

the model outputs the predicted fetch, execution, and store latency of  $\text{Inst}_0$ . We adopt the commonly used rectified linear unit (ReLU) as the activation function of both the convolutional and fully connected layers.

### 3.3 Regression versus Classification

There are multiple ways to connect the ML model output with the predicted latency. A natural scheme is to adopt a *regression* model, i.e., directly using the model output as the predicted latency. In this case, the proposed ML model has three outputs, which correspond to predicted fetch, execution, and store latency, respectively.

One inherited issue for the regression latency prediction model is its inability to distinguish between small latency differences. The impact may be minimal when a latency of 1000 cycles is predicted to be 1001 cycles, but the error could be significant for small latency (e.g., 0 cycle predicted to be 1). Because the fetch latency is 0 or 1 cycle in most cases, this drawback is particularly critical for its prediction. As suggested by Equation 1, a series of small fetch latency prediction errors could accumulate, resulting in a large simulation error for the total program execution time.

A classification model could help to better distinguish between close latency values, where every latency value corresponds to a class, and the ML model predicts which class has the largest probability. However, because the latency could be up to several thousands of cycles, a pure classification scheme will significantly increase the output size and, thus, the computational overhead. Another problem of a pure classification scheme is it is difficult to train such a model due to the lack of training samples with large latency.

**Combining Classification with Regression.** As it is quite expensive to have a class for each possible latency value, we propose a hybrid scheme which uses classification for latency that appears frequently and regression for others. Naturally, small latency appears more frequently. Taking the fetch latency prediction as an example, we classify them into 10 classes in the hybrid scheme. 0 to 8 cycles have dedicated classes ( $c_0, \dots, c_8$ ), while another class is used to represent cycles that are larger than 8 ( $c_{>8}$ ). The proposed model outputs the probability of each class. It also outputs a direct prediction result  $l$  as in the regression model. On a prediction, we first check which class has the largest probability. If it is one among  $c_0, \dots, c_8$ , the corresponding latency is predicted. Otherwise,  $l$  is used as the predicted latency. Similar procedures are used to predict execution and store latency.

### 3.4 Dataset

Due to their data-driven nature, acquiring a sufficiently large training dataset is necessary for the success of ML-based approaches. Fortunately, it is convenient to engage existing simulator infrastructures to acquire a dataset for standard *supervised* training. We modify gem5 [7] to dump instruction execution traces, which then are used to generate ML training/validation/testing datasets.

Table 2 shows the processor configurations that ML models learn from. The default O3CPU resembles a classic super-scalar CPU. We also train models to learn the Fujitsu A64FX CPU deployed in the current top-ranked supercomputer, Fugaku [36, 46], which represents the state-of-the-art CPU. We

Parameter	Default O3CPU	A64FX
Core	3-wide fetch, 8-wide out-of-order issue/commit, bi-mode branch predictor, 32-entry IQ, 40-entry ROB, 16-entry LQ, 16-entry SQ	8-wide fetch, 4-wide out-of-order issue/commit, bi-mode branch predictor, 48-entry IQ, 128-entry ROB, 40-entry LQ, 24-entry SQ
L1 ICACHE	48KB, 3-way, LRU, 4 MSHRs	64KB, 4-way, LRU, 8 MSHRs
L1 DCACHE	32KB, 2-way, LRU, 16 MSHRs, 5-cycle latency	64KB, 4-way, LRU, 21 MSHRs, 8-cycle latency, 8-degree stride prefetcher
I/DMMU	2-stage TLBs, 1KB 8-way TLB caches with 6 MSHRs	2-stage TLBs, 1KB 4-way TLB caches with 6 MSHRs
L2 Cache	1MB, 16-way, LRU, 32 MSHRs, 29-cycle latency	8MB 16-way, LRU, 64 MSHRs, 111-cycle latency

Table 2: Simulated processor configurations.

Type	ML	Simulation
INT	500.perlbench, 502.gcc	505.mcf, 523.xalancbmk, 525.x264, 531.deepsjeng, 548.exchange2, 557.xz, 999.speccrand_i
FP	503.bwaves, 508.namd	507.cactuBSSN, 519.lbm, 521.wrf, 526.blender, 527.cam4, 538.imagick, 544.nab, 549.fotonik3d, 554.roms, 997.speccrand_f

Table 3: Benchmarks for ML and simulation.

obtain the official gem5 configurations of A64FX at [2]. Both processors support the ARMv8 instruction set architecture (ISA), and benchmarks are compiled using gcc 8.2.0 under the O3 optimization level. The full system simulation mode of gem5 is employed with Linux kernel 4.15.

We use the default O3CPU configuration for most of our experiments, while Section 5.4 will present the results for the A64FX configuration. Under the default O3CPU configuration, there are, at most, 110 context instructions. Therefore, the ML model input has  $50 \times (1 + 110) = 5550$  features.

**Benchmark.** Theoretically, any program can be run on the modified gem5 to collect the ML dataset, and we can acquire an unlimited amount of data. We choose to use the SPEC CPU2017 [8] benchmark suite in practice because it includes a wide range of applications, which hopefully lead to a sufficient coverage of instruction execution scenarios. Out of 21 SPEC CPU2017 benchmarks compiled and run in our experimental environment successfully, we select the first four to generate the ML training/validation/testing dataset and leave the remaining 17 benchmarks for simulation testing. Table 3 shows these benchmarks. The default ref inputs are used, and one billion instructions are simulated from the beginning for each benchmark to collect traces. Notably, we use the SPECrate benchmarks while excluding SPECspeed ones due to their similarity.

Because the ML model predicts the latency at the instruction level and most benchmarks use a variety of instructions, benchmark selection for the training set is not critical and can be almost arbitrarily decided. We expect reasonable ML prediction accuracy as long as we collect ample data to cover enough instruction and context scenarios. Section 5.5 will evaluate the impact of training dataset size on prediction accuracy.

**Data Processing.** In the modified gem5, each instruction is assigned with three timestamps to record its respective fetch, execution, and store latency. While the fetch latency stamp is updated in the instruction fetch unit, the execution and store

Model	Output	MFlops	Fetch lat.		Execution lat.		Store lat.		Benchmark simulation error					
			$E_c$	$E_p$	$E_c$	$E_p$	$E_c$	$E_p$	mcf	cactuBSSN	roms	xz	range	abs. avg.
2F	reg	5.69	1.68	57%	3.66	4.3%	2.38	8.4%	21%	16%	28%	20%	[-0.97%, 28%]	18%
3C+2F	reg	8.08	0.76	26%	2.11	2.5%	1.04	3.7%	0.81%	0.59%	1.5%	-0.84%	[-6.6%, 5.2%]	1.9%
5C+2F	reg	21.37	0.48	16%	1.29	1.5%	0.73	2.6%	0.47%	1.7%	1.1%	-0.05%	[-4.6%, 5.5%]	2.0%
7C+2F	reg	50.77	0.50	17%	1.25	1.5%	0.64	2.3%	-2.4%	-0.37%	-1.4%	-4.7%	[-8.7%, 6.3%]	2.5%
7C+2F	hyb	50.8	0.19	6.2%	1.11	1.3%	0.62	2.2%	-0.63%	0.43%	1.3%	-5.5%	[-6.3%, 10.6%]	2.3%
7RB+2F	hyb	93.32	0.15	5.1%	0.96	1.1%	0.52	1.8%	-0.8%	-1.0%	-0.1%	-2.7%	[-2.7%, 0.78%]	0.96%

Table 4: Instruction latency prediction and program simulation accuracy of various ML models. Output indicates if it is a regression model (reg) or hybrid model with classification (hyb). MFlops indicates how many millions of multiplications are required for one inference. Each benchmark is simulated for 10 million instructions.

latency stamps are updated in the ROB and SQ, respectively. After all latency of an instruction is recorded, gem5 dumps it to a trace file.

The instruction traces output by gem5 require several steps of processing before they can be used for ML. First, for each instruction, we find and associate its context instructions based on the timestamps to form a *sample*. Second, many samples may be alike because the same scenarios can appear repeatedly during the execution of benchmarks. We eliminate such duplication to reduce the dataset. Finally, we convert the dataset to a format acceptable by the ML framework used: PyTorch 1.7.0 [27]. On the four SPEC CPU2017 benchmarks used for the ML dataset, the modified gem5 generates 489GB of original trace data, which further converts to 16TB of data with context instructions attached. After data deduplication and conversion, we obtain a 1.5TB dataset with 71 million samples, among which roughly 90% of them are used for training, 5% for validation, and 5% for testing.

### 3.5 Training

We use gradient-based optimization to train various models. Let  $\{(x_i, y_i)\}_{i=1}^n$  represent the set of input and output pairs in our training set of  $n$  items. Let  $f_\theta$  represent a to-be-trained model with parameters  $\theta$ , and our goal is to find a particular  $\theta$  that minimizes the training loss  $J(\theta) = \frac{1}{n} \sum_{i=1}^n L(f_\theta(x_i), y_i)$ .

When training the regression output,  $L$  is the squared-error loss function. When training the classification output,  $L$  is the cross-entropy loss function. Our training code is built upon the PyTorch 1.7.0 library. The objective function  $J$  is minimized using the Adam optimizer [20]. We use a learning rate of 0.001 and no weight decay or momentum. Every model is trained for 200 epochs, and the validation set is used to select the model with the lowest loss.

Our ML training hardware platform is an NVIDIA DGX A100 system [1]. It includes eight NVIDIA A100 GPUs connected through NVLink 3.0 and NVSwitch, and each is equipped with 40GB HBM that supports 1.5 TB/sec peak bandwidth. Tensor cores in an A100 GPU enable a peak performance of 156 TFlops for Tensor Float 32 operations. The DGX A100 system’s high computing and memory throughput make it ideal for ML training and inference. One epoch of training takes between 11 and 23 minutes on the DGX A100 system, depending on the model complexity.

### 3.6 Model Evaluation

We evaluate an array of ML models for instruction latency prediction, and the left part of Table 4 compares their prediction accuracy. For CNNs, C and F represent the respective

convolutional and fully connected layers, and RB denotes the residual block depicted at the bottom of Figure 3. The prefix number represents the number of particular type layers. For example, the 3C+2F model is composed of three convolutional layers followed by two fully connected layers. Due to space limitations, we only list a small fraction of models that have been evaluated.

For every model, we show two prediction errors for each latency type.  $E_c$  represents the average absolute cycle difference between the prediction and truth, i.e.,  $E_c = \text{AVG}(|f_\theta(x_i) - y_i|)$ .  $E_p$  is calculated by dividing the total absolute cycle differences by the total truth cycles, i.e.,  $E_p = \frac{\sum |f_\theta(x_i) - y_i|}{\sum y_i}$ . Based on Equation 1,  $E_p$  of fetch latency is a useful indicator of the program simulation error because  $\sum y_i$  is close to the true simulation time. Section 4.2 will discuss the relationship between latency prediction accuracy and program simulation accuracy in detail. Of note, the normalized error metric is not applicable here because the fetch and store latency (i.e., non stores) is often 0.

Table 4 affords two observations. First, we note that prediction accuracy improves with the number of layers, which demonstrates the necessity of a **deep** neural network. Particularly, 7RB+2F with residual blocks achieves the best accuracy, while the simplest 2F model’s fetch latency  $E_c$  is more than 10 times larger. Second, **classification** helps reduce prediction errors, from 0.50 to 0.19 for fetch latency’s  $E_c$  under 7C+2F, while barely increasing the computation complexity. We notice that with classification, 7C+2F makes correct fetch latency predictions in 96% of cases. In comparison, the regression 7C+2F model predicts 68% of fetch latency correctly, which demonstrates that classification is helpful to predict latency with small values.

## 4. SIMULATOR IMPLEMENTATION

Building on the proposed ML-based instruction latency predictor, we develop a trace-driven computer architecture simulator. The simulator goes through every instruction to predict its latency and outputs the program performance upon completion. The modified gem5 is used to generate input traces. This section will describe other necessary components in the simulator and its parallel GPU implementation.

### 4.1 Context and Clock Management

**Context Management.** The ML predictor requires the features of context instructions as part of its input as introduced in Section 2.4. To this end, we employ two first-in-first-out (FIFO) queues, *processor queue* and *memory write queue*,

to keep track of context instructions that stay in the processor and their features. They roughly correspond to the ROB and SQ in an out-of-order processor but are not exactly the same. The two major differences are that the processor queue includes instructions in the frontend, while ROB does not, and a store instruction enters the memory write queue after it retires from the processor queue.

After the simulator reads one instruction from the input trace, the ML predictor is invoked to predict its latency. Then, it enters the processor queue with the residence latency initialized to 0. When it retires from the processor queue is determined based on its predicted execution latency and other simulation constraints (e.g., it must obey the in-order retirement and retire bandwidth). A non-store instruction exits the simulator when it retires from the processor queue. For a store instruction, it will enter the memory write queue. Similarly, when an instruction retires from the memory write queue is decided based on its predicted store latency, and it will exit the processor at that time. Much like real processors, the retire bandwidth of a processor queue is set according to that of the ROB, and the memory write queue can retire any number of instructions from its tail.

**Clock Management.** The simulator employs `curTick` to record the total number of simulation cycles, which is updated whenever a prediction completes. When the predicted fetch latency is larger than 0, it is added to `curTick` so that the counter always points to the time when the current instruction enters the processor. In this case, we also increase the residence latency of all context instructions by the predicted fetch latency to update the time that they have remained in the processor. When the residence latency of an instruction is larger than its execution latency, it is ready to retire from the processor queue. Similarly, an instruction is ready to retire from the memory write queue when its residence latency exceeds its store latency.

After the last instruction in the input trace is predicted, we continue advancing `curTick` until all instructions retire from the simulator. The final value of `curTick` represents the total execution time of the program, which is exactly the same as Equation 1.

## 4.2 Predictor Accuracy versus Simulation Accuracy

One crucial question that could hamper the success of our ML-based simulation approach involves the relationship between the accuracy of the instruction latency predictor and that of the simulator built upon it. Intuitively, an accurate instruction latency predictor should lead to an accurate simulator. However, because previous prediction results are used to construct the input of latter predictions through the instruction context, the relationship between the predictor’s and simulator’s accuracy is complicated. In the worst-case situation, the prediction errors of instructions can propagate and amplify through the prediction chain, preventing the program simulation from converging. This phenomenon often is referred to as the *compounding error*.

Fortunately, we do not observe such adverse behaviors for our proposed models. We posit that a proper, well-trained ML model, which successfully learns to mimic a processor, can self correct its behaviors throughout the simulation. Such

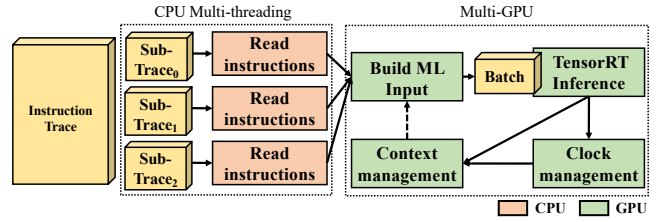


Figure 4: Parallel simulation framework.

self-correction often happens during a real processor’s execution. For example, assume one instruction  $I$  takes longer than it should and prevents the next instruction  $I_n$  from entering the processor earlier. When  $I_n$  enters, the processor pipeline is emptier than it should be, which results in faster execution of  $I_n$ . In such a scenario,  $I$  is executed slower, while  $I_n$  is executed faster. Together, the total execution time self corrects in the right direction. We argue that a sophisticated ML model should be able to learn these self-correction behaviors.

The right side of Table 4 illustrates the program simulation error of various models compared with gem5. It includes the simulation errors for four selective benchmarks (due to space constraints). It also shows the error range and average absolute error for all 17 benchmarks. We simulate 10 million instructions for each benchmark from the beginning. The simulation error  $E_s$  is calculated as  $(CPI_{SIMNET}/CPI_{gem5} - 1) \times 100\%$ , and the average absolute error is  $AVG(|E_s|)$ . Although the instruction prediction accuracy improves significantly from 3C+2F, 5C+2F, and to hybrid 7C+2F models, the simulation errors remain similar. Further improving the instruction prediction accuracy breaks through this simulation accuracy bottleneck as shown in the 7RB+2F model. 7RB+2F achieves the best accuracy and narrowest error range across various models, and its average absolute simulation error is 0.96% across 17 benchmarks. These models represent a variety of **trade-off** points between accuracy and cost. While 7RB+2F is the most accurate model also with the highest computational cost, 3C+2F achieves an acceptable accuracy at a lower cost.

Traditional simulator developers validate the simulator accuracy against the hardware that it intends to simulate. Usually, an error around 10% is considered to be acceptable. For example, ZSim reports an average IPC error of 9.7% against an Intel Westmere CPU [34], and [11] reports a 13% error of gem5 against an ARM Cortex-A15 system. Although we validate the accuracy of SIMNET against gem5 instead of real CPUs, we contend its average absolute error of  $0.96 \sim 2.5\%$  is sufficient to gain confidence about simulation results. Section 5.1 will further validate the simulation accuracy by diving into execution phases.

## 4.3 GPU-accelerated Parallel Simulation

In our ML-based instruction latency predictor, the latency of an instruction depends on the predicted latency of previous instructions, i.e., the latency prediction of adjacent instructions is inherently sequential. This restriction limits the simulation speed, and the sequential SIMNET runs at a throughput around 1k instructions per second. To improve the simulation speed/throughput, we seek to extract parallelism



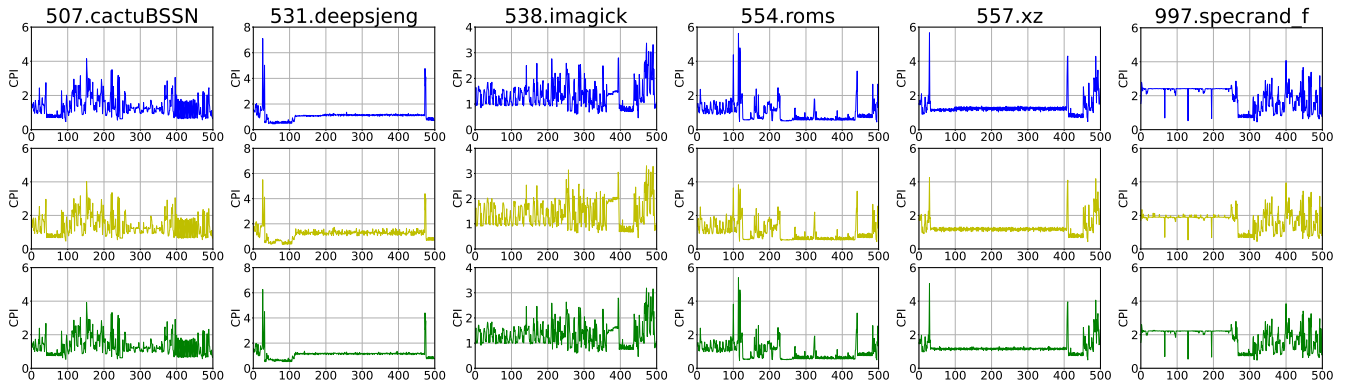


Figure 5: CPI variations during simulation. Each column represents a benchmark. The top row shows the gem5 simulation results, the middle row lists the 3C+2F results, and the bottom row features the 7RB+2F results.

in the sequential simulation.

**Parallel Simulation of Sub-traces.** The primary idea is to break down the input instruction trace into multiple, equally sized continuous sub-traces and to simulate sub-traces in parallel and independently. The drawback of this approach is that extra simulation errors are introduced when simulating head instructions of a sub-trace due to inaccurate contexts. Section 5.2 will show that such accuracy loss is negligible when each sub-trace is large enough.

Figure 4 shows the overview of parallel simulation. The design leverages CPU multi-threading to partition the input trace and transfer sub-trace instructions to the GPU memory in order. The remaining work is done by GPUs to capitalize on their high computational capacity and reduce communications between CPUs and GPUs.

**GPU Acceleration.** Both context and clock management are implemented on GPUs, and each sub-trace has a separate copy of them. Particularly, each sub-trace has its own processor queue and memory write queue, as well a curTick counter to record its number of cycles passed. After the ML model input is built independently for each sub-trace, we combine them into a single input to allow GPU-batched inferences. This process repeats until all instructions in a sub-trace are simulated. After all sub-traces complete their simulation, we sum up their curTicks to get the total execution time.

For ML model inferences, we use TensorRT [42] developed by NVIDIA for high-performance GPU deep learning inferences. It optimizes GPU memory allocations and supports reduced precision inferences. Compared with PyTorch, it provides roughly 4× speedup.

This design can be scaled to multiple GPUs, where each is responsible for a fraction of sub-traces. Section 5.2 will perform a detailed evaluation of simulation throughput.

## 5. EVALUATION

We conduct simulation experiments on our training platform, NVIDIA DGX A100 system equipped with eight A100 GPUs and an AMD EPYC 7742 64-core CPU.

### 5.1 Simulation Phase Validation

To verify the simulation accuracy with respect to execution phases, Figure 5 studies the cycle per instruction (CPI)

variation under 3C+2F and 7RB+2F models for six representative benchmarks, including 997.specrand\_f and 557.xz where they show the largest simulation errors. Particularly, we calculate the average CPI for every 10k simulated instructions and plot these CPIs over a simulation length of 5M instructions (500 points in total). Overall, the CPI curves of SIMNET closely resemble those of gem5, especially those using 7RB+2F. For 538.imagick, 3C+2F’s CPI diverges from that of gem5 between point 360 and 390, while 7RB+2F’s CPI is more similar. We also observe that a period of inaccurate simulation does not impact the simulation accuracy of the time periods that follow. For instance, although 3C+2F does not simulate the first half of 997.specrand\_f accurately, its CPI curve is almost identical to that of gem5 in the second half. The CPI curves of the rest 11 benchmarks show similar observations. These results show that SIMNET not only can predict the overall performance well, but also generate insights about execution phases that cannot be gleaned using approaches such as statistical simulation. As such, these CPI curves can help identify the performance bottleneck.

### 5.2 Parallel Simulation

**Accuracy.** Because the parallel simulator partitions the input trace into multiple sub-traces, there is simulation accuracy loss across sub-trace boundaries. Figure 6 studies how the overall simulation accuracy varies with the number of instructions per sub-trace. It reports the average absolute errors when simulating 100M instructions for 17 benchmarks using three representative models. 7RB+2F cannot have sub-traces that are smaller than 12k instructions because the GPU memory cannot accommodate too many sub-traces. As the results show, the simulation error decreases with an increasing number of instructions per sub-trace. When the sub-trace size is larger than 24k instructions, the parallel simulation error gets close to that of sequential simulation, and the average errors of all three models are below 3%.

**Throughput.** We evaluate the simulation throughput of parallel SIMNET in terms of a million instructions per second (MIPS). Figure 7 evaluates the average throughput across 17 benchmarks with various numbers of sub-traces using the same three models. Increasing the number of sub-traces enables SIMNET to utilize both CPU and GPU resources more

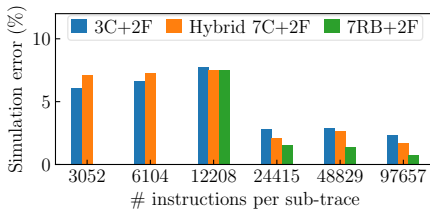


Figure 6: Average parallel simulation errors with various sub-trace sizes.

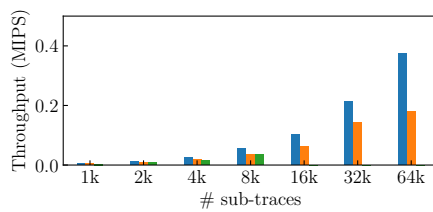


Figure 7: Simulation throughput with different sub-trace numbers.

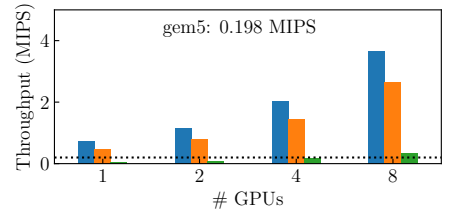


Figure 8: Simulation throughput with multiple GPUs.

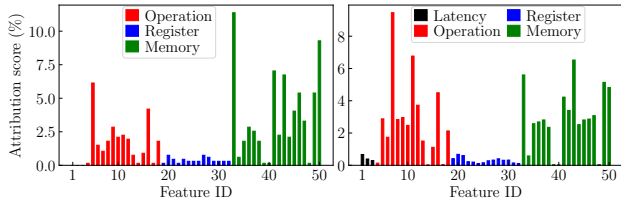


Figure 9: Feature attribution scores.

efficiently until it saturates these resources. 7C+2F enjoys significant throughput improvement until 32k sub-traces, and the lightweight 3C+2F continues benefiting from more sub-traces. We cannot evaluate 3C+2F beyond 64k sub-traces or 7RB+2F beyond 8k sub-traces, limited by the GPU memory capacity.

Figure 8 assesses the throughput scalability of SIMNET with multiple GPUs, where the horizontal black-dotted line marks the gem5 simulation throughput. As ML inferences take a significant portion of time in SIMNET, using multiple GPUs improves both the inference and simulation throughputs. SIMNET achieves near-linear speedup with the number of GPUs. With eight GPUs, it achieves 3.67, 2.63, and 0.34 MIPS with the 3C+2F, hybrid 7C+2F, and 7RB+2F models, respectively, which represent 18.5 $\times$ , 13.4 $\times$ , and 1.7 $\times$  improvement over gem5. We can further scale SIMNET to distributed systems easily for higher throughput.

### 5.3 Impact of Features

Figure 9 evaluates the contribution of each input feature to the ML model output using the SHapley Additive exPlanation (SHAP) method [23]. SHAP computes Shapley values [38] using the coalitional game theory. Shapley value is the average marginal contribution of a feature value across all possible coalitions. We take the average of absolute Shapley values on training samples for each feature to produce feature attribution scores. Figure 9a and 9b summarize the attribution scores of to-be-predicted instructions and context instructions separately. We categorize the 50 features into latency, operation, register, and memory. Memory and operation features generally have more impacts on the prediction results. The most influential feature of to-be-predicted instructions is the fetch access depth, since the fetch latency depends on it. For context instructions, the branch misprediction flag has the largest attribution score, since mispredicted branches need to flush the processor pipeline.

Model	Fetch $E_c$	Execution $E_c$	Store $E_c$	Avg. sim. err.
8C+2F (hyb)	0.24	1.48	0.68	2.2%

Table 5: Model and simulation accuracy for A64FX.

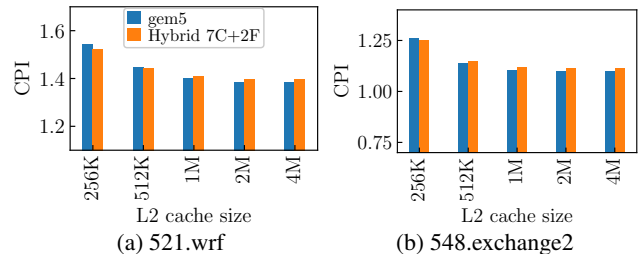


Figure 10: Simulated CPI with various L2 cache sizes.

### 5.4 Architecture Variation

We also evaluate the effectiveness of our ML models under the A64FX configuration. Because A64FX can execute more instructions in parallel, it has 209 context instructions. Table 5 shows the accuracy of the hybrid 8C+2F model after training with the A64FX dataset. It has one additional convolutional layer upon 7C+2F to accommodate more context instructions. Compared with results under the default O3CPU configuration in Table 4, the A64FX model achieves a similar average absolute program simulation error of 2.2% across 17 benchmarks, while instruction prediction errors increase slightly due to the increasing architecture complexity. These results demonstrate that SIMNET also can effectively simulate more complex CPU architectures.

### 5.5 Impact of Training Dataset Size

We also generate a large ML training dataset of 4.5TB using 15 SPEC CPU2017 benchmarks instead of 4. With the hybrid 7C+2F model, using the large dataset further reduces the average simulation error from 2.3% to 1.6%. We conclude that the smaller dataset is enough to train accurate models and also requires less training time.

### 5.6 Case Study: L2 Cache Size Exploration

Figure 10 illustrates the simulated CPI of 521.wrf and 548.exchange2 using gem5 and SIMNET under various L2 cache sizes. Notably, changing cache sizes does not require retraining the model because caches are simulated separately. Compared to gem5, SIMNET shows similar CPI trends. It accurately simulates the performance gain when the L2 cache size increases from 256KB to 1MB, and the tiny improvement from 1MB to 4MB. This experiment demonstrates a use case

of SIMNET for computer architecture research.

## 6. RELATED WORK

**ML for Latency Prediction.** Ithemal [24] uses LSTM models to predict the execution latency of static basic blocks. The instructions within a block are fed into the model in the form of assembly, such as words in NLP. On top of Ithemal, DiffTune [32] trains a differentiable ML performance model to configure the simulator parameters to closely resemble a target architecture. The limits of these methods are they do not consider dynamic execution behaviors, such as memory accesses and branches, which have significant impacts on program performance. They also target basic blocks with a limited number of instructions. As a result, they are not applicable to a computer architecture simulator that needs to execute billions/trillions of dynamic instructions.

**ML for Performance Prediction.** Ipek *et al.* proposes using neural networks for program performance prediction [14]. Meanwhile, Lee and Brooks formulate nonlinear regression models for performance and power prediction [22]. By training a model to learn the performance/power under a limited number of configurations, this work can make predictions under unseen configurations, facilitating design space exploration. Mosmodel [4] is a multi-input polynomial model used for virtual memory research that can predict the program execution time given the page table walking statistics. Some researchers have proposed to predict a processor’s performance/power based on those obtained on different types of processors [5, 6, 26] or with different ISAs [47, 48].

The major difference between these works and our method is that program performance prediction is built upon individual instruction latency predictions in our framework, while these works build performance models on a per program/input basis. As a result, they require retraining models given different programs/input, while our ML-based simulator is able to directly simulate any program, making it much more flexible.

**Simulation with Statistical Sampling.** Instead of simulating the entire program, statistical simulation selectively simulates representative sampling units and infers the overall performance from these sample simulation results statistically [10]. SMARTS [44, 45] periodically switches between detailed and functional simulation to obtain an accurate CPI estimation with minimal detailed simulation. One key challenge in statistical simulation is to keep track of the microarchitecture state between detailed simulation fractions, especially cache states. To simulate the cache behavior accurately in statistical simulation, Nikoleris *et al.* propose using Linux KVM to monitor the reuse distance of selected cache lines [25]. Similarly, Sandberg *et al.* leverage hardware virtualization to fast-forward between samples, so different samples can be simulated in parallel [35]. Compared with our ML-based simulator, these methods cannot extract detailed execution insights, such as the CPI curves in Figure 5. Furthermore, SIMNET and statistical simulation can be used together to further accelerate the detailed simulation portions.

SimPoint records the basic block execution frequencies of individual sampling units and those of the whole program to select representative ones with the aim that the selected samples capture the overall execution behaviors well [31, 39].

Similarly, PinPoints uses dynamic binary instrumentation to find representative samples for X86 programs [29], and BarrierPoint applies sampling to multi-threaded simulation [9]. These methods require pre-analyzing the simulated program with a certain input, while our ML-based simulator can be applied directly to any program and input combination because of its instruction-centric approach.

**ML for Other Architecture Research.** In addition to the aforementioned uses, ML has been widely applied to many other computer architecture aspects, including microarchitecture design and energy/power optimization. Penney and Chen provide a comprehensive survey about ML applications to the computer architecture domain [30].

**Simulation Acceleration.** ZSim is an X86 instruction-driven simulator that supports many-core system simulation [34]. It decouples the simulation of individual cores and resources shared across cores, as well as adopts a simplified core model. As a result, it achieves  $\sim 10$  MIPS for single-thread workload simulation on an Intel Sandy Bridge 16-core processor. SST [16] distributes the simulation of different components across Message Passing Interface (MPI) ranks to achieve parallel simulation. Field programmable gate array (FPGA)-based emulators run significantly faster than software simulators but require a huge amount of effort to develop and validate register-transfer level models [19]. This work addresses accelerating simulation from a different angle to make the most of widely available ML accelerators, such as GPUs.

## 7. CONCLUSIONS

This work proposes a new computer architecture simulation paradigm using ML. To the best of our knowledge, this effort is the first to demonstrate ML’s applicability to full-fledged architecture simulation. The new methodology significantly improves time-to-solution without sacrificing accuracy. In addition to discrete-event, analytical, or other statistical approaches to architectural simulation, we maintain that this new class of simulators will become a useful, valuable addition to the architect’s “bag-of-tools”. We recognize several advantages of this new approach, as well as some limitations.

**Advantages.** 1) We demonstrate that ML-based simulators can predict overall performance accurately, and they also qualitatively capture architecture and application behaviors. 2) ML is intrinsically easier to parallelize than discrete-event simulation. Moreover, ML-based simulators capitalize on modern computing technology that is tailored for boosting ML performance. 3) ML-based simulators generalize well to a large spectrum of application workloads. In our approach, this stems from building them around an instruction-level latency predictor. Hence, the focus is on learning instruction behaviors rather than high-level program behaviors that are much more difficult to capture. 4) The training data are easy and fast to obtain. Potential sources of training data are multiple, including simplified models of simulators, actual execution of code on existing systems, or historical performance data.

**Limitations.** 1) Whereas this first implementation of SIMNET has relatively limited configurability, except caches, TLBs, and branch predictors, we anticipate the expansion to

a full complement of architectural features will not be difficult. 2) More research is required to support the simulation of multi-threaded processors and workloads. Specifically, modeling communication using ML-based simulation is a priority research direction to be tackled.

## REFERENCES

- [1] "Dgx a100: Universal system for ai infrastructure," 2020. [Online]. Available: <https://www.nvidia.com/en-us/data-center/dgx-a100/>
- [2] "Riken simulator for fujitsu a64fx," 2020. [Online]. Available: [https://github.com/RIKEN-RCCS/riken\\_simulator](https://github.com/RIKEN-RCCS/riken_simulator)
- [3] M. Abadi, P. Barham, J. Chen, Z. Chen, A. Davis, J. Dean, M. Devin, S. Ghemawat, G. Irving, M. Isard *et al.*, "Tensorflow: A system for large-scale machine learning," in *12th {USENIX} symposium on operating systems design and implementation ({OSDI} 16)*, 2016, pp. 265–283.
- [4] M. Agbarya, I. Yaniv, J. Gandhi, and D. Tsafir, "Predicting execution times with partial simulations in virtual memory research: why and how," in *IEEE/ACM International Symposium on Microarchitecture (MICRO)*, Global Online Event, October 2020, (to appear).
- [5] N. Ardalani, C. Lestourgeon, K. Sankaralingam, and X. Zhu, "Cross-architecture performance prediction (xapp) using cpu code to predict gpu performance," in *Proceedings of the 48th International Symposium on Microarchitecture*, ser. MICRO-48. New York, NY, USA: Association for Computing Machinery, 2015, p. 725–737. [Online]. Available: <https://doi.org/10.1145/2830772.2830780>
- [6] I. Baldini, S. J. Fink, and E. Altman, "Predicting gpu performance from cpu runs using machine learning," in *2014 IEEE 26th International Symposium on Computer Architecture and High Performance Computing*, 2014, pp. 254–261.
- [7] N. Binkert, B. Beckmann, G. Black, S. K. Reinhardt, A. Saidi, A. Basu, J. Hestness, D. R. Hower, T. Krishna, S. Sardashti, and *et al.*, "The gem5 simulator," *SIGARCH Comput. Archit. News*, vol. 39, no. 2, pp. 1–7, Aug. 2011. [Online]. Available: <https://doi.org/10.1145/2024716.2024718>
- [8] J. Bucek, K.-D. Lange, and J. v. Kistowski, "Spec cpu2017: Next-generation compute benchmark," in *Companion of the 2018 ACM/SPEC International Conference on Performance Engineering*, 2018, pp. 41–42.
- [9] T. E. Carlson, W. Heirman, K. Van Craeynest, and L. Eeckhout, "Barrierpoint: Sampled simulation of multi-threaded applications," in *2014 IEEE International Symposium on Performance Analysis of Systems and Software (ISPASS)*, 2014, pp. 2–12.
- [10] T. M. Conte, M. A. Hirsch, and K. N. Menezes, "Reducing state loss for effective trace sampling of superscalar processors," in *Proceedings International Conference on Computer Design. VLSI in Computers and Processors*, 1996, pp. 468–477.
- [11] A. Gutierrez, J. Pusdesris, R. G. Dreslinski, T. Mudge, C. Sudanthi, C. D. Emmons, M. Hayenga, and N. Paver, "Sources of error in full-system simulation," in *2014 IEEE International Symposium on Performance Analysis of Systems and Software (ISPASS)*, 2014, pp. 13–22.
- [12] K. He, X. Zhang, S. Ren, and J. Sun, "Deep residual learning for image recognition," in *Proceedings of the IEEE conference on computer vision and pattern recognition*, 2016, pp. 770–778.
- [13] S. Hochreiter and J. Schmidhuber, "Long short-term memory," *Neural computation*, vol. 9, no. 8, pp. 1735–1780, 1997.
- [14] E. İpek, S. A. McKee, R. Caruana, B. R. de Supinski, and M. Schulz, "Efficiently exploring architectural design spaces via predictive modeling," in *Proceedings of the 12th International Conference on Architectural Support for Programming Languages and Operating Systems*, ser. ASPLOS XII. New York, NY, USA: Association for Computing Machinery, 2006, p. 195–206. [Online]. Available: <https://doi.org/10.1145/1168857.1168882>
- [15] A. Jaleel, R. S. Cohn, C.-K. Luk, and B. Jacob, "CMPsim: A pin-based on-the-fly multi-core cache simulator," in *Proceedings of the Fourth Annual Workshop on Modeling, Benchmarking and Simulation (MoBS), co-located with ISCA*, 2008, pp. 28–36.
- [16] C. L. Janssen, H. Adalsteinsson, S. Cranford, J. P. Kenny, A. Pinar, D. A. Evensky, and J. Mayo, "A simulator for large-scale parallel computer architectures," *International Journal of Distributed Systems and Technologies (IJ DST)*, vol. 1, no. 2, pp. 57–73, 2010.
- [17] W. Jia, H. Wang, M. Chen, D. Lu, L. Lin, R. Car, W. E, and L. Zhang, "Pushing the limit of molecular dynamics with ab initio accuracy to 100 million atoms with machine learning," in *Proceedings of the International Conference for High Performance Computing, Networking, Storage and Analysis*, ser. SC '20. IEEE Press, 2020.
- [18] N. P. Jouppi, C. Young, N. Patil, D. Patterson, G. Agrawal, R. Bajwa, S. Bates, S. Bhatia, N. Boden, A. Borchers, R. Boyle, P.-I. Cantin, C. Chao, C. Clark, J. Coriell, M. Daley, M. Dau, J. Dean, B. Gelb, T. V. Ghaemmghami, R. Gottipati, W. Gulland, R. Hagmann, C. R. Ho, D. Hogberg, J. Hu, R. Hundt, D. Hurt, J. Ibarz, A. Jaffey, A. Jaworski, A. Kaplan, H. Khaitan, D. Killebrew, A. Koch, N. Kumar, S. Lacy, J. Laudon, J. Law, D. Le, C. Leary, Z. Liu, K. Lucke, A. Lundin, G. MacKean, A. Maggiore, M. Mahony, K. Miller, R. Nagarajan, R. Narayanaswami, R. Ni, K. Nix, T. Norrie, M. Omernick, N. Penukonda, A. Phelps, J. Ross, M. Ross, A. Salek, E. Samadiani, C. Severn, G. Sizikov, M. Snellman, J. Souter, D. Steinberg, A. Swing, M. Tan, G. Thorson, B. Tian, H. Toma, E. Tuttle, V. Vasudevan, R. Walter, W. Wang, E. Wilcox, and D. H. Yoon, "In-datacenter performance analysis of a tensor processing unit," in *Proceedings of the 44th Annual International Symposium on Computer Architecture*, ser. ISCA '17. New York, NY, USA: Association for Computing Machinery, 2017, p. 1–12. [Online]. Available: <https://doi.org/10.1145/3079856.3080246>
- [19] S. Karandikar, H. Mao, D. Kim, D. Biancolin, A. Amid, D. Lee, N. Pemberton, E. Amaro, C. Schmidt, A. Chopra, Q. Huang, K. Kovacs, B. Nikolic, R. Katz, J. Bachrach, and K. Asanović, "Firesim: Fpga-accelerated cycle-exact scale-out system simulation in the public cloud," in *Proceedings of the 45th Annual International Symposium on Computer Architecture*, ser. ISCA '18. IEEE Press, 2018, p. 29–42. [Online]. Available: <https://doi.org/10.1109/ISCA.2018.00014>
- [20] P. D. Kingma and L. J. Ba, "Adam: A method for stochastic optimization," *international conference on learning representations*, 2015.
- [21] A. Krizhevsky, I. Sutskever, and G. E. Hinton, "Imagenet classification with deep convolutional neural networks," *Advances in neural information processing systems*, vol. 25, pp. 1097–1105, 2012.
- [22] B. C. Lee and D. M. Brooks, "Illustrative design space studies with microarchitectural regression models," in *2007 IEEE 13th International Symposium on High Performance Computer Architecture*, 2007, pp. 340–351.
- [23] S. M. Lundberg and S.-I. Lee, "A unified approach to interpreting model predictions," in *Advances in Neural Information Processing Systems 30*, I. Guyon, U. V. Luxburg, S. Bengio, H. Wallach, R. Fergus, S. Vishwanathan, and R. Garnett, Eds., Curran Associates, Inc., 2017, pp. 4765–4774.
- [24] C. Mendis, A. Renda, S. Amarasinghe, and M. Carbin, "Ithelmal: Accurate, portable and fast basic block throughput estimation using deep neural networks," in *International Conference on Machine Learning*. PMLR, 2019, pp. 4505–4515.
- [25] N. Nikolieris, L. Eeckhout, E. Hagersten, and T. E. Carlson, "Directed statistical warming through time traveling," in *Proceedings of the 52nd Annual IEEE/ACM International Symposium on Microarchitecture*, ser. MICRO '52. New York, NY, USA: Association for Computing Machinery, 2019, pp. 1037–1049. [Online]. Available: <https://doi.org/10.1145/3352460.3358264>
- [26] K. O'neal, P. Brisk, A. Abousamra, Z. Waters, and E. Shriver, "Gpu performance estimation using software rasterization and machine learning," *ACM Trans. Embed. Comput. Syst.*, vol. 16, no. 5s, Sep. 2017. [Online]. Available: <https://doi.org/10.1145/3126557>
- [27] A. Paszke, S. Gross, F. Massa, A. Lerer, J. Bradbury, G. Chanan, T. Killeen, Z. Lin, N. Gimelshein, L. Antiga, A. Desmaison, A. Kopf, E. Yang, Z. DeVito, M. Raison, A. Tejani, S. Chilamkurthy, B. Steiner, L. Fang, J. Bai, and S. Chintala, "Pytorch: An imperative style, high-performance deep learning library," in *Advances in Neural Information Processing Systems*, H. Wallach, H. Larochelle, A. Beygelzimer, F. d'Alché-Buc, E. Fox, and R. Garnett, Eds., vol. 32. Curran Associates, Inc., 2019, pp. 8026–8037. [Online]. Available: <https://proceedings.neurips.cc/paper/2019/file/bdbca288fee7f92f2bfa9f7012727740-Paper.pdf>
- [28] A. Patel, F. Afram, S. Chen, and K. Ghose, "Marss: A full system simulator for multicore x86 cpus," in *2011 48th ACM/EDAC/IEEE Design Automation Conference (DAC)*, 2011, pp. 1050–1055.

- [29] H. Patil, R. Cohn, M. Charney, R. Kapoor, A. Sun, and A. Karunanidhi, "Pinpointing representative portions of large intel @ itanium @ programs with dynamic instrumentation," in *37th International Symposium on Microarchitecture (MICRO-37'04)*, Dec 2004, pp. 81–92.
- [30] D. D. Penney and L. Chen, "A survey of machine learning applied to computer architecture design," *arXiv preprint arXiv:1909.12373*, 2019.
- [31] E. Perelman, G. Hamerly, M. Van Biesbrouck, T. Sherwood, and B. Calder, "Using simpoint for accurate and efficient simulation," *SIGMETRICS Perform. Eval. Rev.*, vol. 31, no. 1, pp. 318–319, Jun. 2003. [Online]. Available: <https://doi.org/10.1145/885651.781076>
- [32] A. Renda, Y. Chen, C. Mendis, and M. Carbin, "DiffTune: Optimizing cpu simulator parameters with learned differentiable surrogates," in *IEEE/ACM International Symposium on Microarchitecture*, 2020.
- [33] D. E. Rumelhart, G. E. Hinton, and R. J. Williams, "Learning representations by back-propagating errors," *nature*, vol. 323, no. 6088, pp. 533–536, 1986.
- [34] D. Sanchez and C. Kozyrakis, "Zsim: Fast and accurate microarchitectural simulation of thousand-core systems," *SIGARCH Comput. Archit. News*, vol. 41, no. 3, pp. 475–486, Jun. 2013. [Online]. Available: <https://doi.org/10.1145/2508148.2485963>
- [35] A. Sandberg, N. Nikoleris, T. E. Carlson, E. Hagersten, S. Kaxiras, and D. Black-Schaffer, "Full speed ahead: Detailed architectural simulation at near-native speed," in *2015 IEEE International Symposium on Workload Characterization*, 2015, pp. 183–192.
- [36] M. Sato, Y. Ishikawa, H. Tomita, Y. Kodama, T. Odajima, M. Tsuji, H. Yashiro, M. Aoki, N. Shida, I. Miyoshi, K. Hirai, A. Furuya, A. Asato, K. Morita, and T. Shimizu, "Co-design for a64fx manycore processor and "fugaku"," in *SC20: International Conference for High Performance Computing, Networking, Storage and Analysis*, 2020, pp. 1–15.
- [37] A. W. Senior, R. Evans, J. Jumper, J. Kirkpatrick, L. Sifre, T. Green, C. Qin, A. Židek, A. W. Nelson, A. Bridgland *et al.*, "Improved protein structure prediction using potentials from deep learning," *Nature*, vol. 577, no. 7792, pp. 706–710, 2020.
- [38] L. S. Shapley, "A value for n-person games," *Contributions to the Theory of Games*, vol. 2, no. 28, pp. 307–317, 1953.
- [39] T. Sherwood, E. Perelman, G. Hamerly, and B. Calder, "Automatically characterizing large scale program behavior," in *Proceedings of the 10th International Conference on Architectural Support for Programming Languages and Operating Systems*, ser. ASPLOS X. New York, NY, USA: Association for Computing Machinery, 2002, p. 45–57. [Online]. Available: <https://doi.org/10.1145/605397.605403>
- [40] M. Tan, B. Chen, R. Pang, V. Vasudevan, M. Sandler, A. Howard, and Q. V. Le, "Mnasnet: Platform-aware neural architecture search for mobile," in *Proceedings of the IEEE/CVF Conference on Computer Vision and Pattern Recognition (CVPR)*, June 2019.
- [41] M. Tan and Q. Le, "EfficientNet: Rethinking model scaling for convolutional neural networks," in *Proceedings of the 36th International Conference on Machine Learning*, ser. Proceedings of Machine Learning Research, K. Chaudhuri and R. Salakhutdinov, Eds., vol. 97. PMLR, 09–15 Jun 2019, pp. 6105–6114. [Online]. Available: <http://proceedings.mlr.press/v97/tan19a.html>
- [42] H. Vanholder, "Efficient inference with tensorsrt," 2016.
- [43] A. Vaswani, N. Shazeer, N. Parmar, J. Uszkoreit, L. Jones, A. N. Gomez, Ł. Kaiser, and I. Polosukhin, "Attention is all you need," in *Advances in neural information processing systems*, 2017, pp. 5998–6008.
- [44] T. F. Wenisch, R. E. Wunderlich, M. Ferdman, A. Ailamaki, B. Falsafi, and J. C. Hoe, "Simflex: Statistical sampling of computer system simulation," *IEEE Micro*, vol. 26, no. 4, pp. 18–31, 2006.
- [45] R. E. Wunderlich, T. F. Wenisch, B. Falsafi, and J. C. Hoe, "Smarts: Accelerating microarchitecture simulation via rigorous statistical sampling," in *Proceedings of the 30th Annual International Symposium on Computer Architecture*, ser. ISCA '03. New York, NY, USA: Association for Computing Machinery, 2003, p. 84–97. [Online]. Available: <https://doi.org/10.1145/859618.859629>
- [46] T. Yoshida, "Fujitsu high performance cpu for the post-k computer," in *Hot Chips*, vol. 30, 2018.
- [47] X. Zheng, L. K. John, and A. Gerstlauer, "Accurate phase-level cross-platform power and performance estimation," in *Proceedings of the 53rd Annual Design Automation Conference*, ser. DAC '16. New York, NY, USA: Association for Computing Machinery, 2016. [Online]. Available: <https://doi.org/10.1145/2897937.2897977>
- [48] X. Zheng, P. Ravikumar, L. K. John, and A. Gerstlauer, "Learning-based analytical cross-platform performance prediction," in *2015 International Conference on Embedded Computer Systems: Architectures, Modeling, and Simulation (SAMOS)*. IEEE, 2015, pp. 52–59.